Generation of temperature anisotropy for alpha particle velocity distributions in solar wind at 0.3 AU: Vlasov simulations and Helios observations

D. Perrone, S. Bourouaine, F. Valentini, E. Marsch, P. Veltri

AGU PUBLICATIONS

JGR

Journal of Geophysical Research: Space Physics

RESEARCH ARTICLE

10.1002/2013JA019564

Key Points:
- Comparison between numerical results and observations of temperature anisotropy
- Behavior of the solar wind ions at 0.3 AU for low betas
- Mechanisms for the generation of different shapes of the distribution functions

Correspondence to:
D. Perrone,
denise.perrone@fis.unical.it

Citation:
Perrone, D., S. Bourouaine, F. Valentini, E. Marsch, and P. Veltri (2014), Generation of temperature anisotropy for alpha particle velocity distributions in solar wind at 0.3 AU: Vlasov simulations and Helios observations, *J. Geophys. Res. Space Physics*, *119*, 2400–2410, doi:10.1002/2013JA019564.

Received 23 OCT 2013
Accepted 6 APR 2014
Accepted article online 8 APR 2014
Published online 25 APR 2014

Generation of temperature anisotropy for alpha particle velocity distributions in solar wind at 0.3 AU: Vlasov simulations and Helios observations

D. Perrone[1,2], S. Bourouaine[3], F. Valentini[1], E. Marsch[4,5], and P. Veltri[1]

[1]Dipartimento di Fisica and CNISM, Università della Calabria, Rende, Italy, [2]LESIA, Observatoire de Paris, Meudon, France, [3]Space Science Center, University of New Hampshire, Durham, New Hampshire, USA, [4]Max-Planck-Institut für Sonnensystemforschung, Katlenburg-Lindau, Germany, [5]Institute for Experimental and Applied Physics, Christian-Albrechts-Universität zu Kiel, Kiel, Germany

Abstract Solar wind "in situ" measurements from the Helios spacecraft in regions of the Heliosphere close to the Sun (~0.3 AU), at which typical values of the proton plasma beta are observed to be lower than unity, show that the alpha particle distribution functions depart from the equilibrium Maxwellian configuration, displaying significant elongations in the direction perpendicular to the background magnetic field. In the present work, we made use of multi-ion hybrid Vlasov-Maxwell simulations to provide theoretical support and interpretation to the empirical evidences above. Our numerical results show that, at variance with the case of $\beta_p \simeq 1$ discussed in Perrone et al. (2011), for $\beta_p = 0.1$ the turbulent cascade in the direction parallel to the ambient magnetic field is not efficient in transferring energy toward scales shorter than the proton inertial length. Moreover, our numerical analysis provides new insights for the theoretical interpretation of the empirical evidences obtained from the Helios spacecraft, concerning the generation of temperature anisotropy in the particle velocity distributions.

1. Introduction

The solar wind is the classical paradigm of a collisionless turbulent plasma: this flow of charged particles (electrons, protons, and heavy ions) is hotter than expected for an expanding gas. The observed ion distributions exhibit significant deviations from local thermodynamic equilibrium [*Marsch et al.*, 1982a, 1982b]. Proton distribution functions commonly have features associated with a presence of a beam of accelerated particles along the ambient magnetic field and a perpendicular core temperature anisotropy, whereas the velocity distribution functions of alpha particles mostly reveal isotropic cores.

Wave-particle interactions [*Marsch*, 2006] are thought to play a decisive role in determining the shape of these distribution functions. Moreover, solar wind "in situ" measurements have clearly shown that the alpha particles are preferentially heated and accelerated more than protons [*Kasper et al.*, 2008]. Similar results are obtained from recent numerical hybrid simulations [*Araneda et al.*, 2009; *Ofman and Vinas*, 2007; *Ofman*, 2010; *Maneva et al.*, 2013]. The acceleration of the solar wind and the spatial and temporal evolution of the ion velocity distribution functions are presently some of the key issues of kinetic space physics.

Recently, in order to investigate the physical mechanisms responsible for the complex phenomenology shortly mentioned above, *Bourouaine et al.* [2011a, 2011b] have studied some important parameters (relative speed, temperature ratio, and temperature anisotropy) of alpha particles in the solar wind, benefiting from the detailed proton and alpha particle velocity distribution functions obtained by plasma experiments on the Helios 2 spacecraft. The results described in *Bourouaine et al.* [2011a, 2011b] show that the dynamics of the alpha particles is much more affected by kinetic effects than that of the protons, thus allowing to place new theoretical assumptions on the solar wind models. Moreover, in a recent work, *Verscharen and Marsch* [2011] have analyzed the effect of wave activity on the temperature anisotropy of the ion species in the solar wind, showing that the time-averaging procedure applied in the process of data collection can lead to a generation of an apparent ion temperature anisotropy.

A significant theoretical support for the interpretation of the experimental observations from spacecraft can be provided by kinetic simulations. The fast technological development of supercomputers gives nowadays the possibility of using kinetic Eulerian Vlasov codes [*Mangeney et al.*, 2002; *Valentini et al.*, 2007] that solve

the Vlasov-Maxwell equations in multidimensional phase space. These "low-noise" codes represent an indispensable and crucial tool to investigate the complexity of solar wind physics, since they allow the analysis of kinetic effects in the small-scale tail of the turbulent cascade, where the energy level of the fluctuations is typically very low. In this spectral region, the statistical noise introduced by the Lagrangian Particle In Cell algorithms would crucially affect the numerical results.

Recently, hybrid Vlasov-Maxwell (HVM) simulations in multidimensional phase space configuration [*Valentini et al.*, 2008; *Valentini and Veltri*, 2009; *Valentini et al.*, 2010; *Marradi et al.*, 2010; *Valentini et al.* 2011a, 2011b], in which the Vlasov equation is solved for the proton species while electrons are considered as a fluid, have provided, for the first time, important insights into the nature of the kinetic effects in the tail at short spatial scales of the solar wind turbulent spectra. These numerical results have shown that, regardless of the electron to proton temperature ratio T_e/T_p and for proton plasma beta (β_p) of order unity, a newly identified electrostatic (acoustic-like) branch of fluctuations, called ion-bulk (IBk) waves, seems to represent an efficient channel to carry the energy toward small scales in the longitudinal component of the energy spectra. Moreover, as the result of the turbulent cascade, the proton distribution functions evolve toward a statistical state significantly far from the local thermodynamic equilibrium configuration, due to the resonant interaction of protons with ion-cyclotron waves that leads to the generation of a field-aligned proton beam [see also *Araneda et al.*, 2008; *Maneva et al.*, 2013], whose mean velocity is close to Alfvén speed (V_A).

In 2011, *Perrone et al.* [2011] have extended the HVM code to include the kinetic effects of heavy ions, in order to investigate the role of alpha particles in the kinetic evolution of the solar wind turbulent cascade, in the direction parallel to the ambient magnetic field and in realistic conditions of solar wind at 1 AU (β_p and T_e/T_p of order unity). The first results, in 1D-3V (one dimension in physical space and three dimensions in velocity space) phase space configuration, have reproduced the generation of field-aligned beams (both for protons and alpha particles) along the mean magnetic field and showed that this mechanism of beam production is more efficient for protons than for alpha particles, in agreement with recent solar wind data analysis [*Marsch*, 2012].

More recently, the HVM code, including alpha particles, has been employed in 2D-3V phase space configuration to investigate the ion dynamics at short spatial scales in typical conditions of the solar wind environment at 1 AU. The results mainly consist in the departure of the velocity distributions from the typical Maxwellian configuration under the effect of the turbulence. Preferential perpendicular heating is observed for both ion species, although alpha particles display a more significant anisotropy [*Perrone et al.*, 2013].

In this paper, we present a comparison between the numerical results obtained by a new version of the HVM code, which provides a multi-ion kinetic description, and direct observations of the ion velocity distributions from Helios 2 spacecraft. We simulate a collisionless plasma of kinetic protons and alpha particles and fluid electrons in 1D-3V phase space configuration in situation of decaying turbulence, in which the energy spectra are described over a range of three decades of wave numbers. The goal of the present work is to investigate the behavior of the solar wind ions and the role of kinetic effects on the ion velocity distributions close to the Sun ($\sim$ 0.3 AU) where $\beta_p \ll 1$ [*Tu et al.*, 2004]. The physics of the solar wind plasma appears to be intrinsically related to the values of β_p. Indeed, for the low value of β_p considered here, at variance with the case discussed by *Perrone et al.* [2011] with $\beta_p \simeq 1$, the longitudinal energy cascade is not efficient in transferring energy toward short scales. Moreover, we observed that, while the proton velocity distributions show in general an almost isotropic configuration, significant distortions and elongations are observed for the alpha particle velocity distributions. In agreement with the observational data from the Helios 2 spacecraft, in the HVM simulations alpha particles display evident temperature anisotropy, with a significant elongation in the direction perpendicular to the background magnetic field. The numerical velocity distributions are directly compared to the experimental ones measured by Helios 2, and a physical interpretation of the mechanisms that produce different shapes of the ion distribution functions is provided.

This paper is organized as follows: section 2 presents the HVM model in presence of alpha particles; in section 3 we discuss the numerical results and in section 4 we compare them with observations.

2. Numerical Model

The HVM code integrates numerically the Vlasov equation for the proton (f_p) and alpha particle (f_α) distribution functions. Electrons are treated as a fluid and a generalized Ohm equation, which retains the terms

related to the Hall effect and electron inertia, is employed Faraday equation, Ampere equation (in which the displacement current is neglected), and an equation of state for the electron pressure close the system. Quasi-neutrality is assumed (for details on the set of equations and on the numerical algorithm, see *Valentini et al.* [2007] and *Perrone et al.* [2011]). Here we present the results of simulations in 1D-3V phase space configuration. From now on, times are scaled by the inverse proton-cyclotron frequency Ω_{cp}^{-1}, velocities by the Alfvén speed V_A, lengths by the proton skin depth $d_p = V_A/\Omega_{cp}$ (wave numbers are normalized by d_p^{-1}), and masses by the proton mass m_p.

The initial equilibrium condition consists of a plasma composed of protons and alpha particles with Maxwellian velocity distributions and homogenous density embedded in a background magnetic field $\mathbf{B}_0 = B_0\mathbf{e}_x$ (x is the direction of wave propagation). In order to mimic the initial condition of slab turbulence [*Matthaeus et al.*, 1986], this configuration is perturbed with Alfvénic fluctuations, circularly left-hand polarized in the plane perpendicular to $\mathbf{B}_0$ and propagating along it at wavelengths larger than the proton skin depth. Such Alfvénic fluctuations are represented as a superposition of linearly stationary solutions of the three-fluid equations (for such a range of large wavelengths the system dynamics should be predominantly driven by fluid effects). We inject energy on the first three modes of the spectrum of velocity and magnetic perturbations, in the range of wave numbers $0.078 \leq k \leq 0.23$. If large amplitude perturbations are imposed, nonlinear three-wave coupling should produce a direct energy cascade toward higher wave numbers.

The mathematical form of the imposed perturbations is then given by

$$\begin{cases} \delta u_{y,p} = -\sum_n \epsilon_n \frac{1}{\omega_n - 1} \cos(k_n x) \\ \delta u_{z,p} = -\sum_n \epsilon_n \frac{1}{\omega_n - 1} \sin(k_n x) \end{cases} \tag{1}$$

$$\begin{cases} \delta u_{y,\alpha} = -\sum_n \frac{Z_\alpha m_p}{m_\alpha} \epsilon_n \frac{1}{\omega_n - Z_\alpha m_p/m_\alpha} \cos(k_n x) \\ \delta u_{z,\alpha} = -\sum_n \frac{Z_\alpha m_p}{m_\alpha} \epsilon_n \frac{1}{\omega_n - Z_\alpha m_p/m_\alpha} \sin(k_n x) \end{cases} \tag{2}$$

$$\begin{cases} \delta B_y = -\sum_n \epsilon_n \frac{k}{\omega_n} \cos(k_n x) \\ \delta B_z = -\sum_n \epsilon_n \frac{k}{\omega_n} \sin(k_n x) \end{cases} \tag{3}$$

where ϵ_n is the amplitude of the nth mode and ω_n its frequency [*Perrone et al.*, 2011]. We fix $\epsilon_1 = \epsilon_2 = \epsilon_3 = A/\Delta$, where $A = 0.5$ is the perturbation parameter and Δ is the maximum intensity of all the considered perturbations. This choice provides a $\delta B_{RMS}/B_0 \sim 0.25$, which is in agreement with the observed values for the total wave power at ~0.3 AU [*Bourouaine et al.*, 2010].

Moreover, we choose an isothermal equation of state for the electron pressure P_e and $T_e/T_p = 0.5$. The electron to proton mass ratio is $m_e/m_p = 1/1836$; the alpha particle to proton mass ratio $m_\alpha/m_p = 4$; the alpha particles charge number $Z_\alpha = 2$; the density ratio between alpha particles and protons $n_{0,\alpha}/n_{0,p} = 5\%$; and the alpha particle to proton temperature ratio $T_\alpha/T_p = 1$. No density disturbances are imposed at $t = 0$. As a consequence, the initial Maxwellian ion distribution is

$$f_j(x, \mathbf{v}, t = 0) = K_j(x) n_{0,j} \exp[-(\mathbf{v} - \delta\mathbf{u}_j(x))^2/\beta_j] \tag{4}$$

where $j = p, \alpha$, $K_j(x)$ is such that the velocity integral of f_j gives the equilibrium density $n_{0,j}$ and $\delta\mathbf{u}_j(x)$ is the ion velocity perturbation. Moreover, $\beta_p = 2v_{th,p}^2/v_A^2 = 0.1$ ($v_{th,p} = \sqrt{T_p/m_p} \simeq 0.22$ is the proton thermal speed) and $\beta_\alpha = 0.25\beta_p$. The length of the numerical spatial domain is $L_x \simeq 80 d_p$, while the limits of the velocity domain in each direction are fixed at $v_{p,max} = 11.5 v_{th,p}$ and $v_{\alpha,max} = 23 v_{th,\alpha}$, for protons and alpha particles, respectively. We use 4096 grid points in physical space, where periodic boundary conditions are imposed, and 71^3 and 91^3 grid points in proton and alpha velocity space, respectively. The time step Δt has been chosen in such a way that the Courant-Friedrichs-Lewy condition for the numerical stability of the Vlasov algorithm is satisfied [*Peyret and Taylor*, 1986].

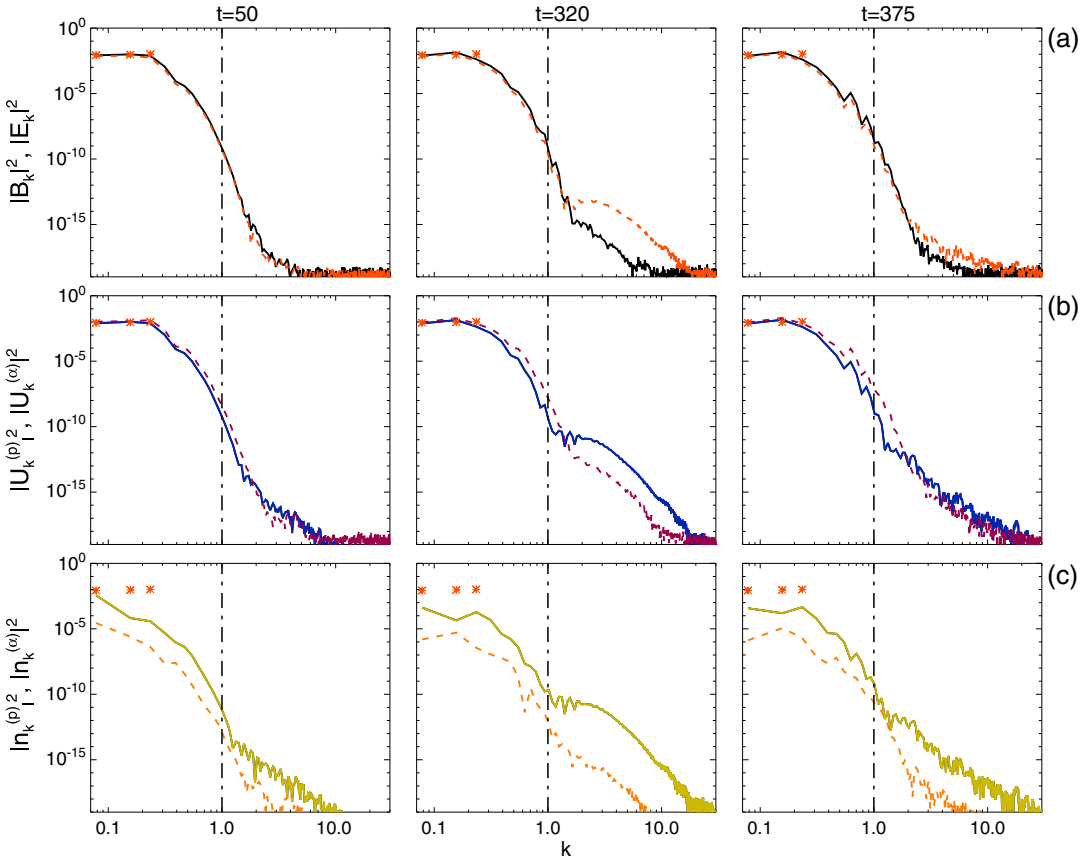

Figure 1. (a) Energy spectra for magnetic (black solid line) and electric (red dashed line) fluctuations. (b) Spectra of proton (blue solid line) and alpha (purple dashed line) kinetic energy. (c) Energy spectra of proton (green solid line) and alpha (orange dashed line) density. In each panel the vertical dash-dotted line indicates the proton skin depth wave number, while the red dots represent the initial wave numbers where the energy is injected at $t = 0$.

3. Numerical Results

Near 0.3 AU, Alfvén cyclotron waves seem to have an important impact on proton perpendicular heating and their resulting temperature anisotropy, connected to the high level of magnetic fluctuations perpendicular to the mean magnetic field [*Bourouaine et al.*, 2010]. We numerically analyze the behavior of protons and alpha particles under the conditions of the plasma close to the Sun. As we will show in detail in the following, the physical scenario pictured by the HVM simulations for low values of the proton plasma beta ($\beta_p = 0.1$) appears significantly different with respect to that described by *Perrone et al.* [2011], for values of β_p of order unity. The reason for this discrepancy is mainly due to the fact that the IBk fluctuations, recovered in the simulations described by *Perrone et al.* [2011], cannot be excited for low values of the proton beta, as explained in *Valentini et al.* [2011b]. As a consequence, for $\beta_p = 0.1$, the energy injected into the system at large scales (larger than d_p) cannot be efficiently transferred to shorter wavelengths (shorter than d_p). In Figure 1 we show the energy spectra for three different times during the simulation ($t = 50$, $t = 320$, and $t = 375$). In Figure 1a, we report the spectra of magnetic (black solid line) and electric (red dashed line) energy: no significant increasing of energy at large wave numbers is recovered in the system. In Figures 1b and 1c, we report respectively the corresponding spectra of proton (blue solid line) and alpha (purple dashed line) kinetic energy; and proton (green solid line) and alpha (orange dashed line) density. As one can easily see from these plots, the energy level at scales smaller than the ion skin depth remains very low. Therefore, the injected energy can be redistributed to the plasma particles, producing distortions of the ion velocity distribution functions.

In Figures 2 and 3 we report the v_x-v_y level lines of the proton and alpha particle distribution functions integrated over v_z and averaged over the entire spatial domain x, for different times in the simulation. For protons (Figure 2), these contour plots display a slight modulation, which consists in a squeezing in the

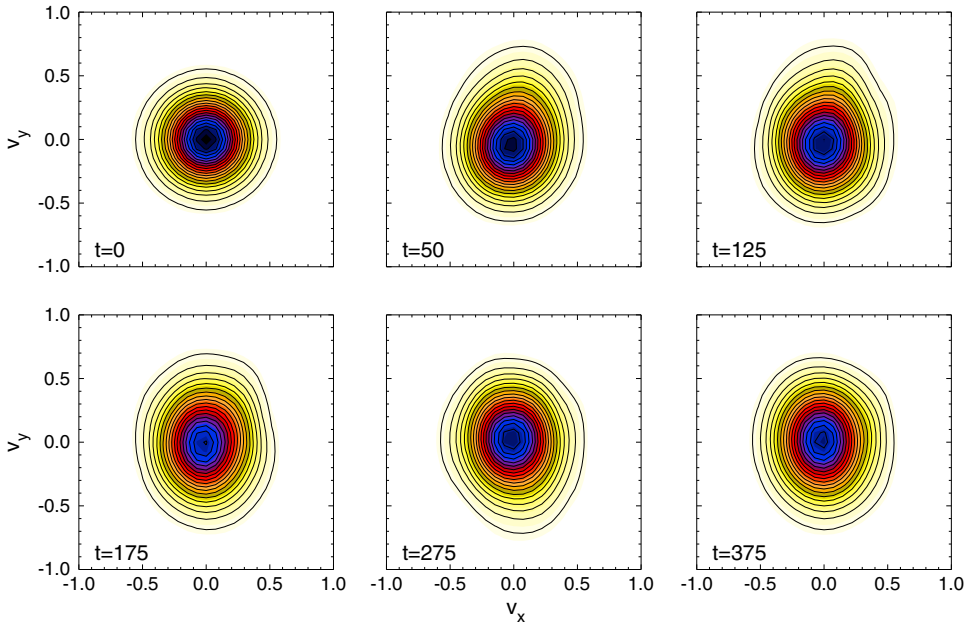

Figure 2. Protons: level lines of the spatial averaged distribution function in the velocity plane v_x-v_y (integrated over v_z) at different times.

direction parallel to the ambient magnetic field and in a consequent perpendicular elongation. In Figure 3, we show the corresponding contour plots for the alpha particle distribution functions. In this case we observe a strong deformation in the direction perpendicular to the ambient magnetic field, with the generation of a beam of accelerated particles.

In order to investigate the particle heating process, in Figure 4 we report the time evolution of the total proton (black solid line) and alpha particle (red dashed line) temperature (averaged on x), normalized to the relative initial values. From this figure, it can be easily seen that the alpha particles are preferentially heated compared to protons. Due to the finite numerical resolution in velocity space and to the low value of the

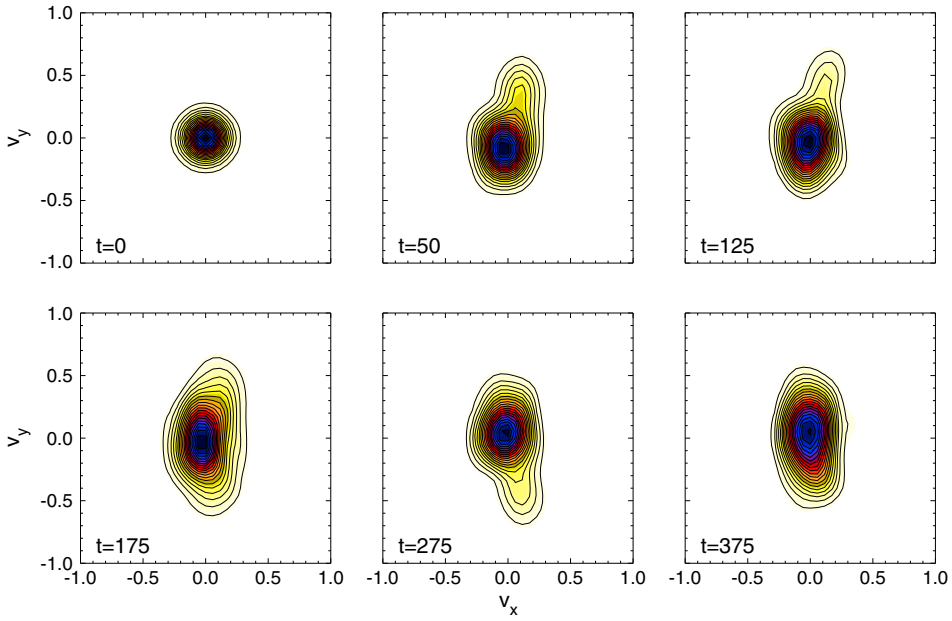

Figure 3. Alpha particles: level lines of the spatial averaged distribution function in the velocity plane v_x-v_y (integrated over v_z) at different times.

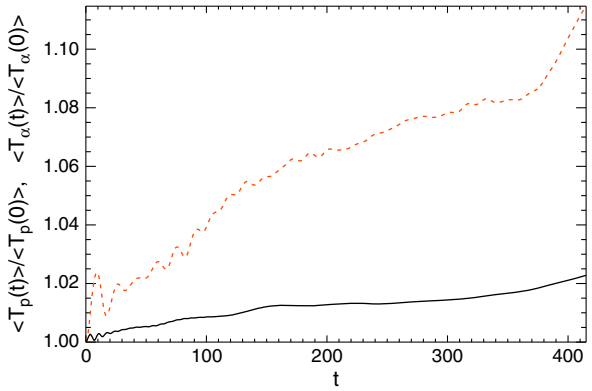

Figure 4. Time evolution of the total proton (black solid line) and alpha particle (red dashed line) temperatures normalized to the initial value and averaged on x. The time is normalized to the inverse of the proton cyclotron frequency.

plasma beta (both for protons and alpha particles), the core of both proton and alpha particle velocity distributions is discretized on a relatively low number of grid points. We point out that the numerical resolution adopted for these simulations is at the limit of the possibilities of the available parallel machines (the simulations have been performed on the FERMI Machine at CINECA, Italy). As a consequence, the entropy of protons and alpha particles (not shown here) displays, during the simulation, an unphysical increase by few percent, due to the low resolution in velocity space. This effect is more relevant for alpha particles than for protons since $v_{th,p} = 2v_{th,\alpha}$. Nevertheless, the conservations of the total energy of the system and of the total mass are highly satisfactory (the relative variation of the total energy is $\simeq 0.06\%$, while that of the total mass is $\simeq 10^{-5}\%$). One can assume that the numerical effect of entropy increase, recovered in our HVM simulations, somehow mimics the expected weak entropy increase owing to the low collisionality of the interplanetary medium at 0.3 AU.

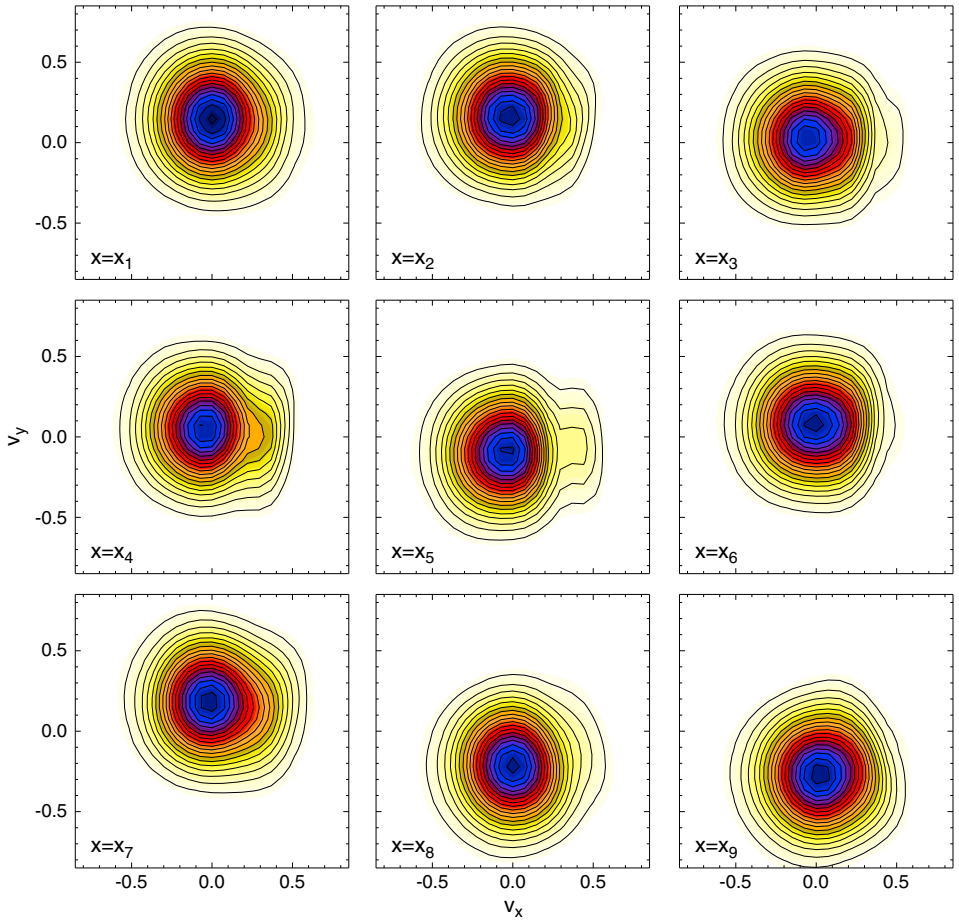

Figure 5. Protons: v_x-v_y level lines of the velocity distribution functions at $t = 375$ for fixed spatial positions ($x_1 \simeq 3$, $x_2 \simeq 12$, $x_3 \simeq 21$, $x_4 \simeq 29$, $x_5 \simeq 37$, $x_6 \simeq 46$, $x_7 \simeq 55$, $x_8 \simeq 64$, and $x_9 \simeq 73$).

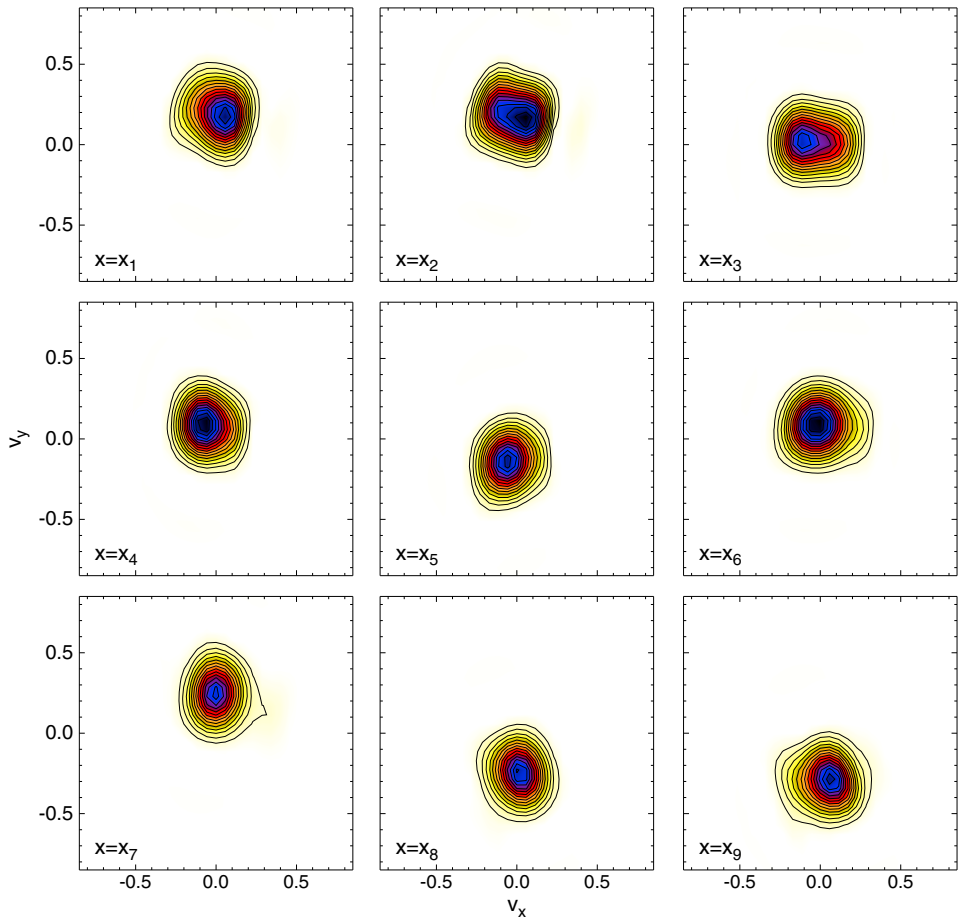

Figure 6. Alpha particles: v_x-v_y level lines of the velocity distribution functions at $t = 375$ for fixed spatial positions ($x_1 \simeq 3$, $x_2 \simeq 12$, $x_3 \simeq 21$, $x_4 \simeq 29$, $x_5 \simeq 37$, $x_6 \simeq 46$, $x_7 \simeq 55$, $x_8 \simeq 64$, and $x_9 \simeq 73$).

Different features appear when one looks at the particle velocity distributions at different spatial positions. In Figure 5 we report the v_x-v_y level lines of the proton distribution at $t = 375$. For given spatial positions (for example, at $x = x_4$ and $x = x_5$), a clear longitudinal elongation is visible. From this figure one can also note a marked oscillation in the direction v_y triggered by the perturbation imposed at $t = 0$ on the initial equilibrium (a similar perpendicular motion is observed in v_z). Figure 6 is the same as Figure 5 for the alpha particle distribution. Here there is no clear tendency of the generation of a longitudinal elongation as observed for the proton velocity distribution in Figure 5; for the alpha particles this elongation can be in any direction depending on the spatial position at which the velocity distribution is considered (see, for example, the longitudinal elongation for $x = x_3$ and $x = x_4$ and the oblique elongation for $x = x_5$ and $x = x_9$).

In order to understand how much the observed perpendicular elongation in the alpha particle velocity distribution is influenced by the spatial numerical discretization, we considered a simple model, in which a distribution function (initially Maxwellian in velocity and homogeneous in space) is perturbed by Alfvenic fluctuations. Using different numbers of excited modes ($N = 1, 3, 10, 25$, and 50) and keeping the same values for the root-mean-square (RMS) of the fluctuations (~0.25), we recovered that, at $t = 400$, the particle distribution function, integrated over v_z and averaged over the entire spatial domain x, displays a strong deformation in the direction perpendicular to the ambient magnetic field, as in the HVM simulations described above. In particular, by evaluating the temperature along the v_y axis for the different cases, we observed that the broadening along the direction perpendicular to the ambient magnetic field depends only on the RMS of the fluctuations and not on the number of the excited modes. This is a robust indication that the limited discretization of our simulation does not affect the genuineness of the physical results.

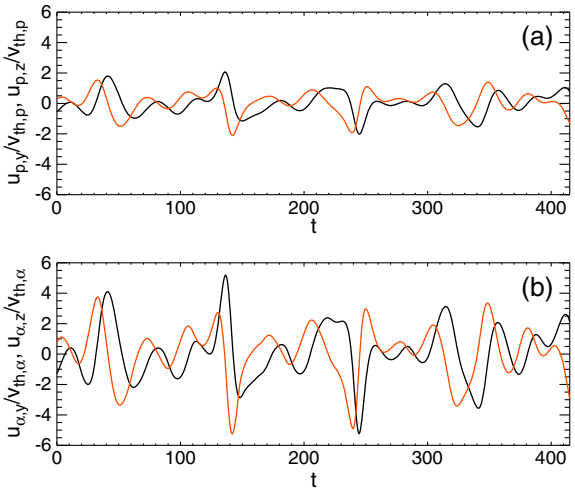

Figure 7. Time evolution of the y (black) and z (red) components of the mean velocity (evaluated at $x = x_5$ and normalized to the particle thermal speed) for (a) protons and (b) alpha particles. The time is scaled by the inverse of the proton cyclotron frequency.

In Figure 7 we report the time evolution of the components of the particle mean velocities perpendicular to the direction of the mean magnetic field, evaluated in a spatial position $x = x_5$, $u_{i,j}(x_5, t) = \int v_j f_i(x_5, \mathbf{v}) \mathrm{d}^3\mathbf{v}/n_i$ ($i = p, \alpha$ and $j = y, z$), normalized to the particle thermal speed $v_{\mathrm{th},i}$. In Figure 7a we show the mean velocities for protons (y component in black and z component in red), while in Figure 7b the same quantities are reported for alpha particles. As one can easily see from Figure 7, the amplitude of the mean velocity oscillations for alpha particles δU_α is almost 6 times larger than $v_{\mathrm{th},\alpha}$, while for the protons δU_p is about 2 times larger than $v_{\mathrm{th},p}$. We point out that the amplitude of the longitudinal fluctuations of the bulk velocity both for protons and alphas is almost 1 order of magnitude lower than the amplitude of the corresponding transverse fluctuations. The numerical evidences reported in Figure 7 will be discussed in detail in the next section in relation to the observational data from Helios 2.

4. Observations

In this section we provide some measurements of the velocity distribution function (VDF) of alpha particles done by Helios 2 during its first perihelion passage in 1976. The Helios plasma experiment measures the ion energy distribution at different azimuth and elevation angles within 10 s (time it takes to step through the relevant energy channels, mostly only 9), but the plasma measurement cadence was about 40 s. However, the three-dimensional ion analyzer does not separate the energy distribution of the proton core (which is the major species) from the alpha particles and proton beam. Therefore, in order to separate the alpha particle energy distribution, we determine the relative minima and maxima in the combined ion energy. The VDF of alpha particles can be identified once the maximum which is related to the proton beam is determined. This separation method can also be verified by comparing the simultaneous measurements of the particle and charge count rate spectra. Indeed, the ratio of the charge to particle fluxes at the maximum (which corresponds to the alpha particle VDF) is about 2 times the ratio at the maximum which is related to the proton VDF peak, [e.g., *Marsch et al.*, 1982a, 1982b]. The method of separating alpha VDFs from the total observed ion spectra is robust, and it reduces enormously any contribution from proton cores or even proton beams to the alpha particle VDFs.

In Figure 8 we display the contour plots of the measured alpha particle VDFs in (**V**,**B**) plane. Here $\mathbf{V}$ is the solar wind flow velocity vector and $\mathbf{B}$ is the background magnetic field vector. The alpha VDFs (or the reduced alpha VDFs) that are displayed in Figure 8 are obtained through the integration of the full 3D VDFs over the transverse velocity component to the plane (**V**,**B**) or (**x**,**B**) since **V** ∥ **x** (**x** direction toward the Sun). The integration over the transverse velocity component is performed after interpolating alpha particle VDFs (which initially were measured in the spacecraft frame and in a spherical coordinate system) in alpha particle moving frame. It turns out that the contours of the inner part of alpha particle VDFs are roughly symmetric, but far from the core, the contours are no longer symmetric and are mainly elongated across the ambient magnetic field to one side more than the other. However, the sharp edges at the very tail end of the alpha VDFs are artifacts of the interpolation on the coarse velocity grid. This shape of the alpha particle VDF is mostly obtained for low-proton plasma beta ($\beta_p \sim 0.1$). Therefore, the Maxwellian shape for alpha particle VDFs is not always maintained in low plasma beta. Moreover, the proton core VDFs are mainly elongated across the background magnetic field displaying a clear perpendicular heating with ($T_\perp > T_\parallel$) [e.g., *Marsch et al.*, 1982a; *Bourouaine et al.*, 2010, 2011b].

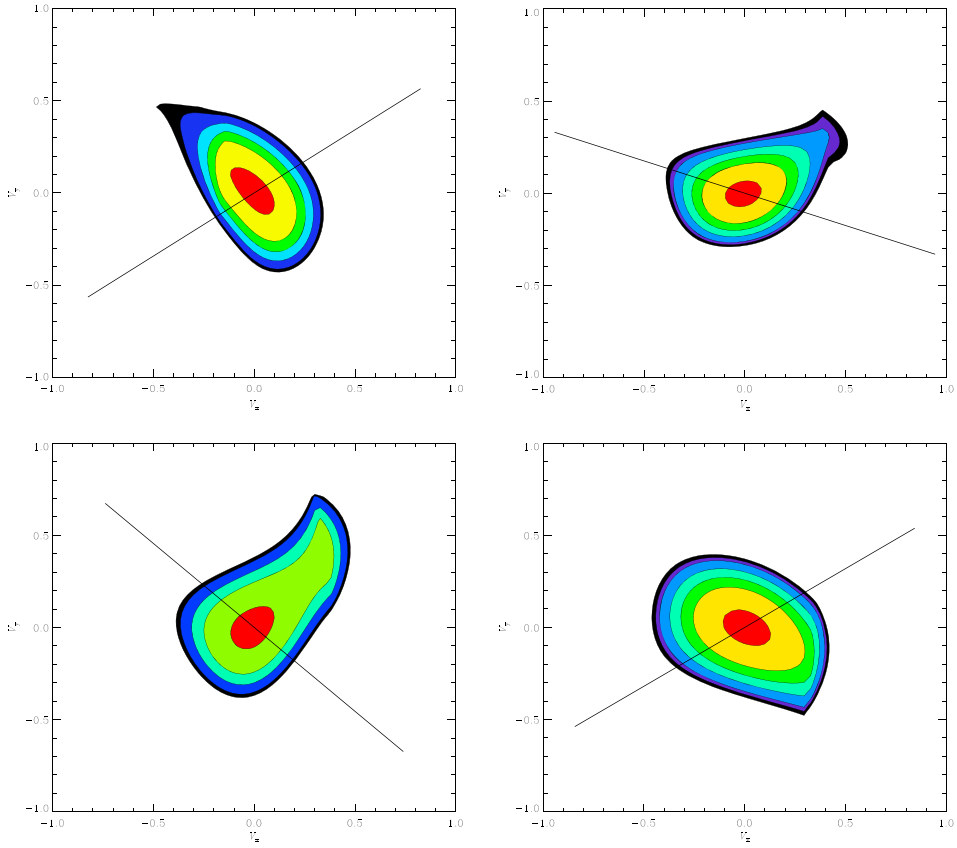

Figure 8. Contour plots of alpha particle VDFs in (**V**,**B**) plane measured by Helios 2 at the Heliocentric distance, $R = 0.29$ AU. The direction x points towards the Sun. The straight line represents the orientation of the background magnetic field. The values of the proton plasma beta that correspond to the measurements of these VDFs are all about 0.1. The normalized VDF values that are higher than 0.98 with respect to the maximum are represented by red color, and the normalized VDF values which are ranging between [0.9,0.98], [0.85,0.90], [0.80,0.85], [0.750.,80], [0.73,0.75], and [0.73,0.70] are represented by yellow, green, light green, blue, violet, and dark colors, respectively.

The simulation results of alpha particles given in section 3 (Figure 3) show a clear temperature anisotropy for the VDFs of alpha particles integrated over the whole space of the simulation box (i.e., $80d_p$). Moreover, their shapes show a broadening along the direction perpendicular to **B** although the VDFs given at fixed time and space position appear to be cooler (Figure 6). Therefore, relying on the integrated VDFs, we are led to believe that the alpha particles are perpendicularly heated.

The Vlasov simulation may explain the observed temperature anisotropy for alpha particle VDFs in low plasma beta regions. According to the simulation, the existence of transverse waves (even with relatively small amplitude) can lead to an oscillation transverse drift of alpha particles whose oscillating amplitude is $\delta U_\alpha > v_{\mathrm{th},\alpha}$ (where $v_{\mathrm{th},\alpha}$ is the local thermal speed of alpha particles), as it is clearly seen in Figure 6. Therefore, when we average or integrate the VDF over the space then the coherent motion (even at relatively large scales) may cause a broadening in the integrated VDF. We would expect that those effects do not occur when the oscillating drift is much smaller than the local ion thermal speed $\delta U \leq v_{\mathrm{th},i}$. According to Figure 5 the displacement of the proton VDFs in velocity space, δU_p, is relatively smaller than the local proton thermal speed, i.e., $\delta U_p \simeq v_{\mathrm{th},p}$. Therefore, the distortion effect on the integrated proton VDF is negligible, as it is clear from Figure 2, and thus the Maxwellian shape can be maintained.

For the measurements of the ion VDFs, the plasma experiment does not provide a snapshot of the VDF at a given time and space position, but rather it gives an integrated VDF within the measurement time which is about 10 s. If we consider the typical values of solar wind speed, $V \sim 700$ km s^{-1}, and the proton inertial length, $d_p \sim 100$ km, then the 10 s time period would correspond to a measurement distance of about $70d_p$. Therefore, in low plasma beta condition, the integrated VDF of alpha particles or other minor ions can be affected even by large-scale fluctuations. The presence of such fluctuations may cause an apparent

broadening in the VDF. However, one would expect that such effect on the alpha particles and minor ions VDFs could be reduced when the measurement time is smaller than 10 s.

The future space missions of Solar Orbiter and Solar Probe Plus might provide high-resolution plasma measurements, and thus the microphysics of alpha particles and the other minor ions can be studied with high accuracy in low plasma beta regions.

5. Summary and Conclusions

In the turbulent collision-free solar wind, as observed "in situ" by many spacecraft and simulated in several numerical experiments, the velocity distributions of ions generally exhibit significant non-Maxwellian features [*Marsch et al.*, 1982a, 1982b; *Kasper et al.*, 2008], such as the generation of beams of accelerated ions [*Marsch et al.*, 1982a, 1982b; *Marsch*, 2012] or the production of temperature anisotropy [*Bourouaine et al.*, 2010, 2011a, 2011b; *Verscharen and Marsch*, 2011].

In this paper, we analyzed in detail the evolution of the distribution functions of the solar wind protons and alpha particles along the development of the turbulent energy cascade in the direction parallel to the background magnetic field, in the typical conditions of the interplanetary medium at 0.3 AU from the Sun. The analysis has been performed by means of a Eulerian HVM code [*Valentini et al.*, 2007; *Perrone et al.*, 2011] that numerically solves the Vlasov equation for the distribution function of protons and alpha particles, in presence of fluid isothermal electrons. Moreover, evidences for the occurrence of temperature anisotropy for the velocity distributions of alpha particles obtained from the Helios 2 spacecraft have been presented and discussed in relation to the numerical results.

Even though the initial setup of the simulations has been designed in such a way that both the ion species have Maxwellian distributions of velocities at $t = 0$, during the system evolution kinetic processes drive the plasma away from the condition of thermodynamic equilibrium. Looking at the contour plots of the numerical particle distributions in the velocity plane, in which one axis corresponds to the direction of the ambient magnetic field, suggests a physical interpretation for the measurement of the alpha velocity distributions from Helios 2.

In fact, when the numerical distribution function is averaged in physical space over the entire spatial domain, the velocity level lines of f_α display the generation of a marked temperature anisotropy, revealing significant elongations in the direction perpendicular to the background magnetic field (see Figure 3). These numerical structures well reproduce the typical shapes of the alpha velocity distributions found in the Helios 2 measurements (see Figure 8).

As we have discussed in detail in the previous section, the perpendicular deformation of the numerical alpha particle velocity distributions (when averaged in space) is due to the fact that the mean velocity of the alpha species displays evident oscillations in the direction perpendicular to $\mathbf{B}_0$ (triggered by the initial perturbation), whose amplitude becomes larger than the particle thermal speed $v_{\mathrm{th},\alpha}$; therefore, the process of spatial averaging evidently produces perpendicular broadening. On the other hand, when the same velocity level lines are analyzed in a fixed spatial location (no spatial average), the alpha particle velocity distributions remain mostly Maxwellian (see Figure 6). It is worth to point out that the process of averaging applied during the data collection by Helios 2 in fact corresponds to the spatial average performed in the simulations. At variance with the case of alpha particles, for the protons the oscillation amplitude of the perpendicular bulk velocity is almost comparable to the particle thermal speed $v_{\mathrm{th},p}$. As a consequence, the proton velocity distributions remain mainly Maxwellian when f_p is spatially averaged (see Figure 2).

The comparison between the numerical results and the observational data discussed in the present paper allows us to provide a possible physical interpretation to the generation of temperature anisotropy in the velocity distributions of heavy ions at low plasma beta. According to this interpretation, the apparent perpendicular broadening of the alpha particle velocity distributions, as recovered both in the numerical simulations and in the Helios 2 observations, can be explained as being due to sampling and averaging, which were applied during the reduction of the measured and simulated data. Recent analyses on solar wind data from the Wind spacecraft are along the lines of our work. In fact, Maruca and Kasper in 2013 [*Maruca and Kasper*, 2013] revisited previously published results on ion temperature anisotropy in the solar wind [*Kasper et al.*, 2002], pointing out how time-averaging procedures can generate the artificial effect of blurring the perpendicular and parallel temperature components of the ion velocity distributions.

Acknowledgments
Numerical simulations were performed on the FERMI supercomputer at CINECA (Bologna, Italy) within the European project PRACE Pra04-771. This work was supported in part by NASA grant NNX11AJ37G at the University of New Hampshire.

Philippa Browning thanks the reviewers for their assistance in evaluating this paper.

References

Araneda, J. A., E. Marsch, and A. F. Vinas (2008), Proton core heating and beam formation via parametrically unstable Alfvén-cyclotron waves, *Phys. Rev. Lett.*, *100*, 125003.

Araneda, J. A., Y. Maneva, and E. Marsch (2009), Preferential heating and acceleration of α particles by Alfvén-cyclotron waves, *Phys. Rev. Lett.*, *102*, 175001.

Bourouaine, S., E. Marsch, and F. M. Neubauer (2010), Correlations between the proton temperature anisotropy and transverse high-frequency waves in the solar wind, *Geophys. Res. Lett.*, *37*, L14104, doi:10.1029/2010GL043697.

Bourouaine, S., E. Marsch, and F. M. Neubauer (2011a), On the relative speed and temperature ratio of solar wind alpha particles and protons: Collisions versus wave effects, *Astrophys. J.*, *728*, L3–L7.

Bourouaine, S., E. Marsch, and F. M. Neubauer (2011b), Temperature anisotropy and differential streaming of solar wind ions. Correlations with transverse fluctuations, *Astron. Astrophys.*, *536*, A39.

Kasper, J. C., A. J. Lazarus, and S. P. Gary (2002), WIND/SWE observations of firehose constraint on solar wind proton temperature anisotropy, *Geophys. Res. Lett.*, *29*(17), 1839, doi:10.1029/2002GL015128.

Kasper, J. C., A. J. Lazarus, and S. P. Gary (2008), Hot solar-wind helium: Direct evidence for local heating by Alfvén-cyclotron dissipation, *Phys. Rev. Lett.*, *101*, 261103.

Maneva, Y. G., A. F. Vinas, and L. Ofman (2013), Turbulent heating and acceleration of He^{++} ions by spectra of Alfvén-cyclotron waves in the expanding solar wind: 1.5-D hybrid simulations, *J. Geophys. Res. Space Physics*, *118*, 2842–2853, doi:10.1002/jgra.50363.

Mangeney, A., F. Califano, C. Cavazzoni, and P. Trávníček (2002), A numerical scheme for the integration of the Vlasov-Maxwell system of equations, *J. Comput. Phys.*, *179*, 495–538.

Marradi, L., F. Valentini, and F. Califano (2010), Kinetic evolution of the perpendicular turbulent cascade in the solar wind, *Europhys. Lett.*, *92*, 49002.

Marsch, E., K.-H. Mühlhäuser, H. Rosenbauer, R. Schwenn, and F. M. Neubauer (1982a), Solar wind protons: Three-dimensional velocity distributions and derived plasma parameters measured between 0.3 and 1 AU, *J. Geophys. Res.*, *87*(A1), 52–72.

Marsch, E., K.-H. Mühlhäuser, R. Schwenn, H. Rosenbauer, W. Pilipp, and F. M. Neubauer (1982b), Solar wind helium ions: Observations of the Helios solar probes between 0.3 and 1 AU, *J. Geophys. Res.*, *87*(A1), 35–51.

Marsch, E. (2006), Kinetic physics of the solar corona and solar wind, *Living Rev. Sol. Phys.*, *3*, 1.

Marsch, E. (2012), Helios: Evolution of distribution functions 0.31 AU, *Space Sci. Rev.*, *172*, 23.

Maruca, B. A., and J. C. Kasper (2013), Improved interpretation of solar wind ion measurements via high-resolution magnetic field data, *Adv. Space Res.*, *52*, 723–731.

Matthaeus, W. H., M. L. Goldstein, and J. H. King (1986), An interplanetary magnetic field ensemble at 1 AU, *J. Geophys. Res.*, *91*, 59–69, doi:10.1029/JA091iA01p00059.

Ofman, L., and A. F. Vinas (2007), Two-dimensional hybrid model of wave and beam heating of multi-ion solar wind plasma, *J. Geophys. Res.*, *112*, A06104, doi:10.1029/2006JA012187.

Ofman, L. (2010), Hybrid model of inhomogeneous solar wind plasma heating by Alfvén wave spectrum: Parametric studies, *J. Geophys. Res.*, *115*, A04108, doi:10.1029/2009JA015094.

Perrone, D., F. Valentini, and P. Veltri (2011), The role of alpha particles in the evolution of the solar-wind turbulence toward short spatial scales, *Astrophys. J.*, *741*, 43.

Perrone, D., F. Valentini, S. Servidio, S. Dalena, and P. Veltri (2013), Vlasov simulations of multi-ion plasma turbulence in the solar wind, *Astrophys. J.*, *762*, 99.

Peyret, R., and T. D. Taylor (1986), *Computational Methods for Fluid Flow*, Springer-Verlag, New York, Heidelberg, Berlin.

Tu, C.-Y., E. Marsch, and Z.-R. Qin (2004), Dependence of the proton beam drift velocity on the proton core plasma beta in the solar wind, *J. Geophys. Res.*, *109*, A05101, doi:10.1029/2004JA010391.

Valentini, F., P. Trávníček, F. Califano, P. Hellinger, and A. Mangeney (2007), A hybrid-Vlasov model based on the current advance method for the simulation of collisionless magnetized plasma, *J. Comput. Phys.*, *225*, 753–770.

Valentini, F., P. Veltri, F. Califano, and A. Mangeney (2008), Cross-scale effects in solar-wind turbulence, *Phys. Rev. Lett.*, *101*, 025006.

Valentini, F., and P. Veltri (2009), Electrostatic short-scale termination of solar-wind turbulence, *Phys. Rev. Lett.*, *102*, 225001.

Valentini, F., F. Califano, and P. Veltri (2010), Two-dimensional kinetic turbulence in the solar wind, *Phys. Rev. Lett.*, *104*, 205002.

Valentini, F., F. Califano, D. Perrone, F. Pegoraro, and P. Veltri (2011a), New ion-wave path in the energy cascade, *Phys. Rev. Lett.*, *106*, 165002.

Valentini, F., D. Perrone, and P. Veltri (2011b), Short-wavelength electrostatic fluctuations in the solar wind, *Astrophys. J.*, *739*, 54.

Verscharen, D., and E. Marsch (2011), Apparent temperature anisotropies due to wave activity in the solar wind, *Ann. Geophys.*, *29*, 909–917.